IJBPAS, May, 2026, 15(5): 2008-2030

ISSN: 2277–4998

International Journal of Biology, Pharmacy and Allied Sciences (IJBPAS)

'A Bridge Between Laboratory and Reader'

www.ijbpas.com

DEVELOPMENT AND CHARACTERIZATION OF LANSOPRAZOLE NANOSPONGES FOR ENHANCED SOLUBILITY AND CONTROLLED DRUG RELEASE

PATEL A* AND PATEL R

Ramanbhai Patel College of Pharmacy, Charotar University of Science and Technology (CHARUSAT), CHARUSAT Campus, Changa-388421, India

***Corresponding Author: Dr. Adil Patel: E Mail: Adilpatel.ph@charusat.ac.in**

Received 25th Jan. 2025; Revised 24th March 2025; Accepted 28th May 2025; Available online 1st May 2026

https://doi.org/10.31032/IJBPAS/2026/15.5.9465

ABSTRACT

This study presents the preparation and characterization of Lansoprazole nanosponges using soluble chitosan, polyvinyl alcohol (PVA), and Pluronic F68 via the emulsion solvent diffusion method. The nanosponges were formulated to enhance the drug's solubility and controlled release profile. Differential Scanning Calorimetry (DSC) confirmed the transition of Lansoprazole to an amorphous state, indicating uniform distribution within the nanosponge matrix. Scanning Electron Microscopy (SEM) revealed spherical, porous nanosponges. Dynamic Light Scattering (DLS) analysis showed an average particle size of 332.4 nm with a moderate polydispersity index (PDI) of 0.52, while zeta potential measurements indicated moderate stability with a value of -15.3 mV. Fourier-transform infrared (FTIR) spectroscopy confirmed the entrapment of Lansoprazole without significant interactions with the polymers. The in vitro drug release study demonstrated a controlled and sustained release profile, achieving nearly complete drug release over 11 hours. These findings suggest that the prepared Lansoprazole nanosponges possess the desired characteristics for potential therapeutic applications, offering improved solubility, stability, and a controlled release mechanism.

Keywords: Lansoprazole, Nanosponges, Soluble Chitosan, Polyvinyl Alcohol (PVA), Pluronic F68, Emulsion Solvent Diffusion, Controlled Release, Differential Scanning Calorimetry (DSC), Scanning Electron Microscopy (SEM), Dynamic Light Scattering (DLS), Zeta Potential

INTRODUCTION:

Recently many researchers have shown interest in developing drug loaded nanosponges due to their ability to be a promising controlled release drug delivery system. Due to its ability to control the release rates of drug at targeted sites drug loaded nanosponges are making significant contribution to the health care system. Nanosponges have advantages like high stability, high carrier capacity and compatibility towards both hydrophilic and hydrophobic substances. The main limitation of nanosponges is their ability to include only small molecules **[1]**. The sponge is a three dimensional network or scaffold. The long length polyester acts as the backbone. These long length polyesters are mixed in solution with cross linkers to form the polymer. The result of this chemical reaction is the formation of spherically shaped particles filled with cavities for the entrapment of drugs. The biodegradable polymer matrix breaks down slowly in body fluids and thus releases loaded drug in a predictable fashion. It is possible to synthesise nanosponges with specific size and release profile by taking different rations of crosslinker to polymer. Nanosponges are small spherical shaped solid particles with a porous surface. They can be formulated as oral, parenteral, topical and/or inhalation dosage forms. However the limitation of nanosponges is its ability to entrap only small molecules **[2]**.

lansoprazole, a proton pump inhibitor is prescribed widely in the treatment of gastric ulcer, gastro oesophageal reflux disease, duodenal ulcer, ulcers associated with usage of nonsteroidal anti inflammatory drug and long term management of zollinger-ellison syndrome. It is mainly metabolised by the liver. Due to this there is a need to reduce the dose for patients suffering from hepatic failure. However such reduction of dose in the conventional dosage form may result in less or no therapeutic effect. Side effects associated with regular use of lansoprazolee include abdominal pain, diarrhoea, skin rashes, thrombocytopenia, impotence etc. hence there is a need to develop a controlled release drug delivery system of lansoprazole. Buccal route is preferred in this study for advantages like safety, comfort, reliability and direct absorption in systemic circulation by avoiding hepatic metabolism **[3]**.

MATERIAL AND METHOD:

Lansoprazole was provided as a sample by Dr. Reddy's Labs Limited, Hyderabad. Carboxymethyl Chitosan, Polyvinyl Alcohol, and Pluronic F68 were obtained from Qualigens Fine Chemicals, New Delhi. All other ingredients used were of analytical grade.

Methodology:

Preparation of lansoprazole nanosponges:

Lansoprazole nanosponges were prepared using varying ratios of Carboxymethyl Chitosan, polyvinyl alcohol, and Pluronic F68 via the emulsion solvent diffusion method. The disperse phase, which included 100 mg of lansoprazole and a specified amount of Carboxymethyl Chitosan dissolved in 30 mL of dichloromethane, was gradually added to a defined quantity of PVA in 100 mL of the aqueous continuous phase. This mixture was stirred at 1000 rpm using a magnetic stirrer for two hours. The resulting lansoprazole nanosponges were then collected through vacuum filtration and dried in an oven at 40°C for 24 hours **[4]**.

Percentage yield:

After drying, the lansoprazole nanosponges were weighed. The percentage yield was calculated using the following formula:

% yield = (Weight of nanosponges × 100) / Total weight of solids [5].

Entrapment efficiency:

The entrapment efficiency of lansoprazole nanosponges was determined using a UV spectrophotometric method. A calibration curve for lansoprazole in methanolic HCl was created within the range of 3-18 µg/mL (Beer's Lambert range) at 293 nm. The relationship between lansoprazole concentration and its absorbance was highly linear ($r^2 = 0.9993$, m = 0.0469, n = 3). For each batch, 100 mg of lansoprazole nanosponges were selected, powdered in a mortar, and placed in 100 mL of methanolic HCl. The lansoprazole was extracted by centrifugation at 1000 rpm for 30 minutes, filtered, and its concentration was analyzed using the calibration curve after appropriate dilution. The percentage entrapment efficiency was calculated using the formula:

% Entrapment Efficiency = (Actual drug content in the nanosponge × 100) / Theoretical drug content [6]

Particle size measurement:

The average particle size of lansoprazole nanosponges was measured using photon correlation spectroscopy (PCS) with a Nano ZS-90 instrument (Malvern Instruments Ltd, UK) at a constant angle at 25°C. The sample was diluted tenfold with distilled water before particle size analysis **[7]**.

Zeta potential:

The zeta potential was measured to determine the movement velocity of the particles in an electric field and their charge. In this study, the nanosponges were diluted tenfold with distilled water and analyzed using a Zetasizer with Laser Doppler Micro-electrophoresis (Zetasizer Nano ZS, Malvern Instruments Ltd., UK) **[8]**.

Particle shape and morphology:

The shape and morphology of the nanosponges were investigated using Scanning Electron Microscopy (LEO 440I).

The sample was placed on a glass slide and kept under vacuum. It was then coated with a thin layer of gold/palladium using a sputter coater. The scanning electron microscope was operated at an acceleration voltage of 15 kV **[9]**.

Fourier transform infrared spectroscopy studies:

FTIR spectral measurements were conducted at room temperature using a Perkin Elmer Model 1600 (USA). The samples were mixed with KBr powder, and pellets were formed by applying a pressure of 5 tons. The FTIR spectra were obtained using powder diffuse reflectance on an FTIR spectrophotometer **[10]**.

Differential scanning calorimetric studies:

Differential scanning calorimetry (DSC-60, Shimadzu Corporation, Japan) was performed to assess the compatibility between the drug and polymers. After calibration with indium and lead standards, samples (3-5 mg) were heated in crimped aluminum pans from 50°C to 400°C at a rate of 10°C/min under a nitrogen atmosphere. The enthalpy of fusion and melting point were calculated automatically **[11]**.

Porosity:

The bulk volume was measured by pouring the nanosponges into a graduated cylinder. After recording this initial volume, the cylinder was tapped 100 times, and the resulting volume was noted as the true volume. The percentage porosity was calculated using the formula: **% Porosity = [(Bulk Volume - True Volume) / Bulk Volume] × 100**. **[12]**

Determination of residual solvents concentration:

Gas chromatography (Shimadzu GC-14B chromatograph, Japan) was employed to estimate the residual dichloromethane in lansoprazole nanosponges. The dichloromethane content was analyzed using an Agilent 7890 Gas Chromatograph (USA) equipped with a flame ionization detector. To estimate residual solvents, 100 mg of nanosponges were dissolved in a small amount of DMSO in a 10 mL volumetric flask, then diluted to 10 mL with DMSO. The solution was filtered through a 0.45 µm filter and degassed using a sonicator. A 1 µL sample was injected into the chromatograph, the chromatogram was recorded, and the solvent peak area was measured. A calibration curve for dichloromethane was plotted in the range of 10-50 ppm, showing a good linear relationship between the concentration of dichloromethane and its peak area (r^2=0.9989). The concentration of residual solvent was calculated using the calibration curve data **[13]**.

Preparation of lansoprazole buccal film:

LPZ -loaded nanosponge buccal films were fabricated through the solvent casting method, utilizing mucoadhesive polymers that are capable of forming films. An accurate weighing of 2% w/v of hydroxypropyl methylcellulose E15 (HPMC) was followed by dissolution in 2 ml of ethanol. The polymer and ethanol mixture in the beaker was allowed to rest for a duration of 5 minutes to facilitate polymer swelling. An additional quantity of 3 ml of ethanol was introduced into the aforementioned polymer solution, and the resulting mixture was subjected to stirring. Subsequently, a minute quantity of propylene glycol, weighing 0.029 g, was introduced into the polymer solution. Concurrent LPZ-loaded nanosponges equivalently were precisely measured to yield a dosage of 15 mg per 2 cm^2 of film and subsequently dissolved in 1 ml of ethanol in a separate vessel. The polymer solution was subjected to the addition of the drug solution and homogenized using a magnetic stirrer. The entire solution was transferred into a glass petri dish that was positioned on a level surface. A device in the form of an inverted funnel was positioned atop the dish in order to prevent abrupt vaporization.

In vitro drug release study:

In-vitro drug release of nanosponge-loaded buccal film formulation was studied by dialysis method. The amount of drug released was measured using uv-spectrophotometer and the graph of % cumulative drug release vs time (mins) was plotted, it was found that nanosponge loaded buccal film formulation showed slower drug release for around 8 hours **[14]**.

RESULTS & DISCUSSION:

The melting point of a substance is a critical property that indicates its purity and identity. In this study, the melting point of the Lansoprazol was determined using two different methods: the Capillary Fusion Method and Differential Scanning Calorimetry (DSC). The Capillary Fusion Method reported a melting point range of 178-181°C. Upon conducting the experiment, the observed melting point was found to be 179-181°C. This close agreement between the reported and observed melting points suggests that the sample is of high purity. DSC is a more advanced technique that provides precise thermal analysis, and the observed melting point range confirms the findings from the Capillary Fusion Method. The observed melting point range of 179-181°C was consistent across both methods, demonstrating the reliability of the data. The slight variation between the reported melting point (178-181°C) in the Capillary Fusion Method and the observed melting

points is minimal and within an acceptable range.

Infrared (IR) spectroscopy is a powerful analytical technique used to identify functional groups and molecular interactions within a sample. In this study, the IR spectra of pure lansoprazole and a physical mixture of lansoprazole with excipients were compared to assess any potential interactions between the drug and excipients. The comparison between the IR spectra of pure lansoprazole and the physical mixture reveals that the primary functional groups of lansoprazole remain intact in the presence of excipients. The absence of significant shifts or disappearance of characteristic peaks suggests that there are no strong chemical interactions between lansoprazole and the excipients in the physical mixture. This indicates that the excipients do not affect the structural integrity of lansoprazole, which is crucial for maintaining its pharmacological activity.

The experiment aimed to evaluate the effects of varying amounts of two polymers (Factor 1: Polymer A and Factor 2: Polymer B) on three response variables: particle size (in nm), polydispersity index (PDI), and encapsulation efficiency (EE, in %). The particle size increased with the amount of Polymer A across all levels of Polymer B. For instance, at 900 g of Polymer B, increasing Polymer A from 400 g to 1000 g resulted in an increase in particle size from 329.7 nm to 779.8 nm. Similarly, at 1200 g of Polymer B, increasing Polymer A from 400 g to 1000 g led to a rise in particle size from 415.6 nm to 978.4 nm. The smallest particle sizes were observed with the lowest amount of Polymer A (400 g) regardless of the amount of Polymer B used. The trend suggests that the particle size is primarily influenced by the amount of Polymer A. Higher amounts of Polymer A likely contribute to increased viscosity and particle agglomeration, leading to larger particle sizes.

The PDI values varied but showed some trends. Lower PDI values (indicating more uniform particle size distribution) were generally observed with lower amounts of Polymer B. For instance, with 600 g of Polymer B, PDIs were 0.52, 0.61, and 0.63 for increasing amounts of Polymer A. Higher PDIs, indicating a broader particle size distribution, were often seen at higher amounts of Polymer B. For example, at 1200 g of Polymer B, the PDIs were 0.86, 0.89, and 0.88 for increasing amounts of Polymer A. The PDI results suggest that higher amounts of Polymer B lead to less uniform particle sizes, possibly due to the increased likelihood of forming aggregates or variations in the polymer matrix. Lower amounts of Polymer B seem to favor more uniform particle distribution.

The encapsulation efficiency (EE) showed a general trend of increasing with the amount of Polymer A when the amount of Polymer B was constant. For example, at 900 g of Polymer B, increasing Polymer A from 400 g to 1000 g increased EE from 64.59% to 72.81%. However, the highest EE observed (72.81%) was not significantly higher than the EEs observed at lower amounts of Polymer A and B. The EE varied with Polymer B but did not show as clear a trend as with Polymer A. For example, at 400 g of Polymer A, varying Polymer B from 600 g to 1200 g decreased EE from 62% to 53.79%. The encapsulation efficiency appears to be more sensitive to the amount of Polymer A. Higher amounts of Polymer A might provide better encapsulation due to increased available surface area and interaction sites for encapsulation. However, there is a point where increasing Polymer A does not significantly improve EE, indicating a possible saturation point. The data indicates that the amount of Polymer A has a significant impact on particle size, PDI, and EE. Increasing Polymer A generally leads to larger particle sizes and improved encapsulation efficiency but can also result in less uniform particle size distributions when combined with higher amounts of Polymer B. The amount of Polymer B influences PDI more strongly, with higher amounts leading to broader particle size distributions.

The table presents statistical metrics for different regression models (Linear, Two-Factor Interaction (2FI), Quadratic, and Cubic) used to fit the experimental data. The Linear model demonstrates a good fit with an R^2 value of 0.9474, indicating that approximately 94.74% of the variance in the data is explained by the model. The adjusted R^2 (0.9299) is slightly lower, which is expected as it adjusts for the number of predictors in the model. The predicted R^2 (0.8597) is also reasonably high, suggesting that the model has good predictive power. The relatively low PRESS value supports the model's adequacy. These metrics collectively suggest that the Linear model provides a good balance between fit and simplicity, making it a suggested model for the data. Among the models evaluated, the Linear model appears to be the most appropriate choice based on the balance of fit and predictive power. It has a high R^2 and adjusted R^2, and a reasonably high predicted R^2 with the lowest PRESS value, indicating good generalizability to new data. The 2FI, Quadratic, and Cubic models, despite showing higher R^2 values, suffer from overfitting as evidenced by their lower predicted R^2 values and higher PRESS values. Therefore, the Linear model is suggested for use in this analysis.

The ANOVA results indicate that both factors, the amount of Polymer A (CMC) and the amount of Polymer B (PVA), significantly influence the response variable. Factor A has a stronger effect compared to Factor B, as evidenced by its higher sum of squares and F-value. The overall model is highly significant, demonstrating that the selected factors are appropriate for explaining the variability in the response. These findings suggest that optimizing the amounts of these polymers can effectively control the response variable in the formulation process.

(PDI) The model summary statistics indicate that the model provides a strong and reliable fit to the data. The high R^2 and adjusted R^2 values demonstrate that the model explains a significant portion of the variance in the response variable. The predicted R^2 indicates good predictive ability, while the low standard deviation and coefficient of variation suggest precise predictions. The high adequate precision value confirms that the model has a strong signal relative to noise. Overall, these metrics collectively suggest that the model is robust, reliable, and well-suited for predicting the response variable based on the factors studied.

The ANOVA results indicate that the interaction between Polymer A and Polymer B (AB) and the quadratic term for Polymer B (B^2) are statistically significant. The interaction term (AB) has a significant effect on the response variable, suggesting that the combination of these polymers plays an important role in influencing the outcome. The quadratic effect of Polymer B is also significant, indicating a strong curvature effect. In contrast, the quadratic effect of Polymer A is not significant, suggesting that the response variable does not exhibit a significant curvature effect with respect to Polymer A within the studied range.

These findings highlight the importance of considering both the interaction and quadratic effects of the polymers when optimizing the formulation to achieve the desired response. The model fits the data well, as indicated by the low residual sum of squares and the overall statistical significance of the relevant terms.

The DLS results indicate that the sample has an average particle size (Z-average diameter) of 332.4 d.nm with a moderate polydispersity index (PdI) of 0.52. The intercept value of 0.669 suggests good data quality. The size distribution by intensity shows a single peak at 290.9 d.nm with 100% intensity, indicating that the majority of particles are around this size, but there is some variability as shown by the standard deviation of 166.8 d.nm. Overall, the sample is characterized by moderately uniform particles with good quality measurements.

The zeta potential analysis results indicate that the sample has a moderate negative zeta potential of -15.3 mV, suggesting incipient instability with some potential for particle aggregation over time. The zeta deviation of 6.96 mV indicates moderate variability in particle surface charge, which can impact stability. The conductivity is low at 0.0560 mS/cm, supporting the observed zeta potential by minimizing counterion effects. The single peak in the zeta potential distribution confirms the uniformity of the surface charge across the sample.

Overall, while the sample shows reasonable stability, the moderate zeta potential indicates that it may require additional stabilization measures for long-term stability. The good quality rating of the results ensures that these findings are reliable and can be used to inform further formulation or stability enhancement efforts.

The SEM analysis of formulation F4 revealed the presence of porous, spherical, and nanoscale particles. The figure provides a clear representation of the porous and spongy nature of the nanosponges.

The Fourier-transform infrared (FTIR) spectrum of formulation batch F4 indicates the absence of significant functional peak displacement. Furthermore, the sharp peaks of the drug exhibit a decrease in intensity, suggesting that the drug has been entrapped.

The DSC thermogram of pure LPZ is shown in comparison to the optimized nanosponge formulation in the figure 24. The purity of LPZ was demonstrated by a endothermic melting peak, which was compatible with data in the literature. The drug melting peak was not visible on the DSC thermogram of the optimized Nanosuspension formulation (figure 24), and no other new peaks appeared, indicating that the drug had changed to an amorphous state. Loss of drug crystallinity also indicated uniformity of drug distribution within the matrix, which could be attributed to the presence of surfactant, which inhibits drug crystallization.

Dichloromethane was used as an organic solvent to dissolve the drug. It belongs to class two solvent and can be used in the pharmaceutical formulation with a limit of 600 ppm. The sample was analysed with respect to the dichloromethane used in the preparation and the amount of dichloromethane was found to be 453.68 ppm which is considered to be safe and within the range.

During the initial 3 hours, the %CDR increases gradually from 10.584% to 25.985%. This phase likely represents the initial burst release, where the drug on or near the surface of the delivery system is quickly released into the surrounding medium. Between 3 to 5 hours, there is a

marked increase in %CDR, reaching up to 60.214%. This accelerated release phase indicates that the drug is being released at a higher rate, potentially due to the dissolution or diffusion mechanisms of the delivery system. From 5 to 9 hours, the %CDR continues to increase but at a slightly reduced rate, reaching 90.548%. This phase suggests a more controlled and sustained release, which is often desired in drug delivery systems to maintain therapeutic levels of the drug over an extended period. In the final phase from 9 to 11 hours, the %CDR reaches near completion, with 99.452% released by 11 hours. This indicates that most of the drug has been released, and the system has effectively delivered the drug over the specified period. The cumulative drug release data indicates a well-defined release profile with distinct phases: an initial burst release, an accelerated release, a sustained release, and a final release phase. The drug delivery system appears to be effective in releasing the drug gradually over an 11 hour period, achieving almost complete release by the end of the study. The low standard deviations suggest that the release data is reliable and reproducible.

The in vitro drug release profile from the buccal patch demonstrates a well-defined release pattern characterized by an initial burst release, followed by an accelerated release phase, and then a sustained release phase, culminating in near-total drug release by the 8th hour. The consistency in the data, as indicated by the small standard deviations, supports the reliability of the measurements.

This release profile is advantageous for therapeutic applications requiring both an initial rapid onset of action and sustained drug delivery to maintain therapeutic levels. The effective delivery of nearly 100% of the drug within 8 hours suggests that the buccal patch formulation is efficient and suitable for potential clinical use.

Table 1: Determination of melting point

Method	Reported Melting Point	Observed Melting Point
Capillary Fusion Method	**178-181°C**	**179-181°C**
Differential Scanning Calorimetry		**179-181°C**

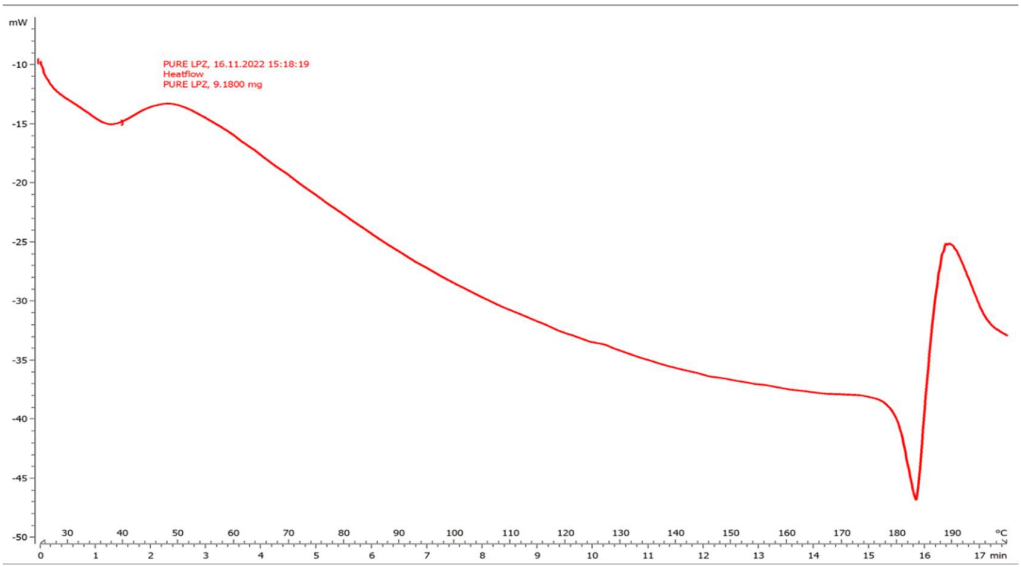

Figure 1: DSC graph of lansoprazole

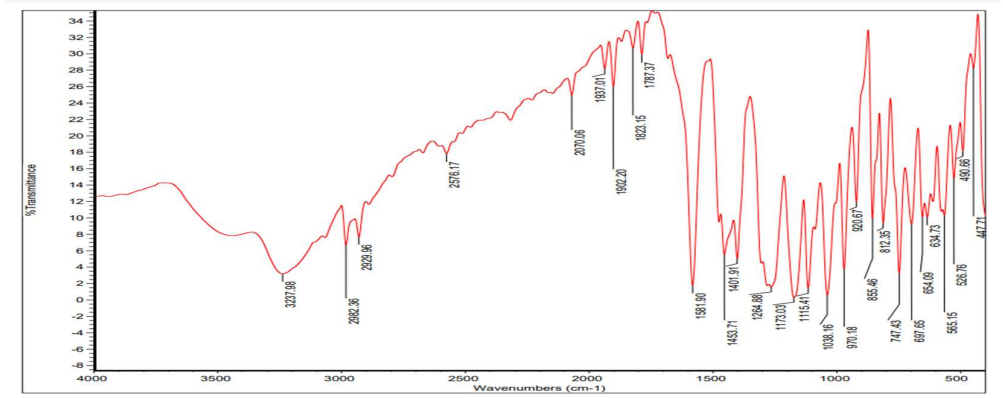

Figure 2: FTIR spectra of Lansoprazole

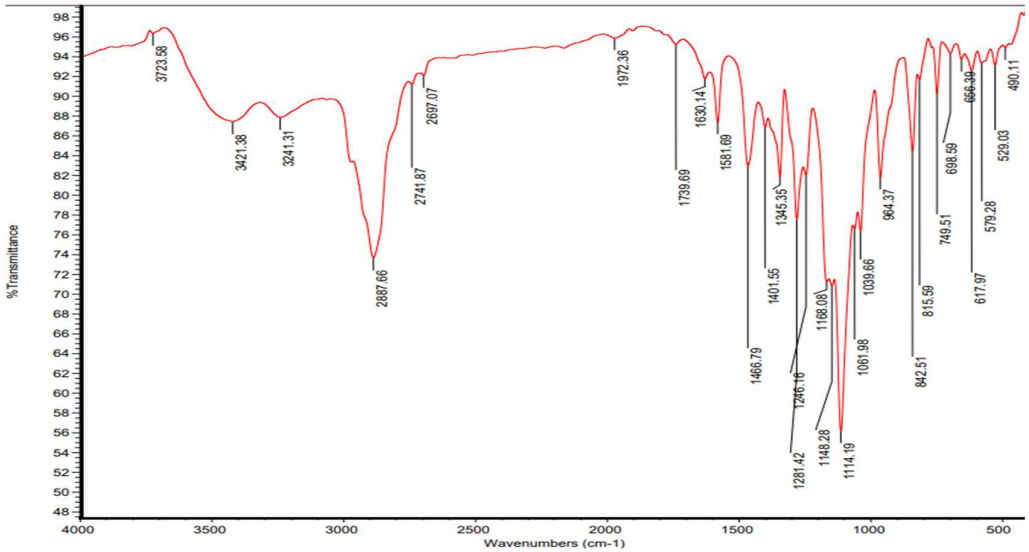

Figure 3: FTIR spectra physical mixture

Table 2: Results of experimental batches

Run	Factor 1	Factor 2	Response 1	Response 2	Response 3
	A: amount of polymer a (gm)	B: amount of polymer b (gm)	Particle size Nm	PDI	EE %
1	400	900	329.7 ± 23.58	0.73 ± 0.21	64.59 ± 5.23
2	700	900	572.6 ± 32.14	0.75 ± 0.11	70.28 ± 4.28
3	1000	900	779.8 ± 12.35	0.69 ± 0.32	72.81 ± 9.54
4	400	600	332.4 ± 32.86	0.52 ± 0.14	62 ± 5.21
5	400	1200	415.6 ± 12.42	0.86 ± 0.18	53.79 ± 3.52
6	700	1200	698.2 ± 15.74	0.89 ± 0.20	60.23 ± 4.98
7	1000	1200	978.4 ± 10.68	0.88 ± 0.10	68.76 ±5.33
8	700	600	396.8 ± 36.54	0.61 ± 0.31	65 ± 6.42
9	1000	600	752.4 ± 26.87	0.63 ± 0.23	67 ± 5.26

Table 3: Results of the different models for particle size

Source	Std. Dev.	R^2	Adjusted r^2	Predicted r^2	Press	
Linear	61.17	0.9474	0.9299	0.8597	59872.38	Suggested
2fi	58.92	0.9593	0.9349	0.7639	1.008e+05	
Quadratic	61.53	0.9734	0.9290	0.7157	1.213e+05	
Cubic	60.03	0.9916	0.9324	-0.5390	6.568e+05	Aliased

Table 4: ANOVA data for particle size

Source	Sum of squares	Df	Mean square	F-value	P-value	
Model	4.043e+05	2	2.022e+05	54.02	0.0001	Significant
A-cmc	3.422e+05	1	3.422e+05	91.44	< 0.0001	
B-pva	62138.73	1	62138.73	16.60	0.0065	
Residual	22453.48	6	3742.25			
Cor total	4.268e+05	8				

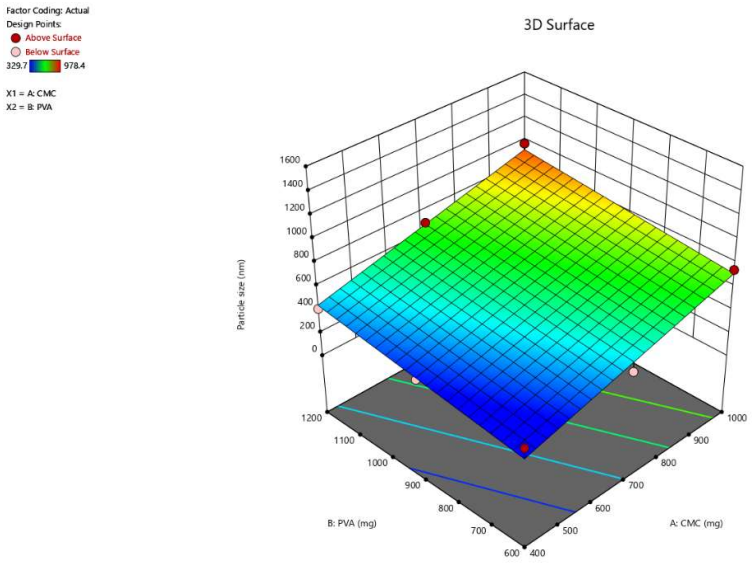

Figure 4: the 3d surface plot of particle size

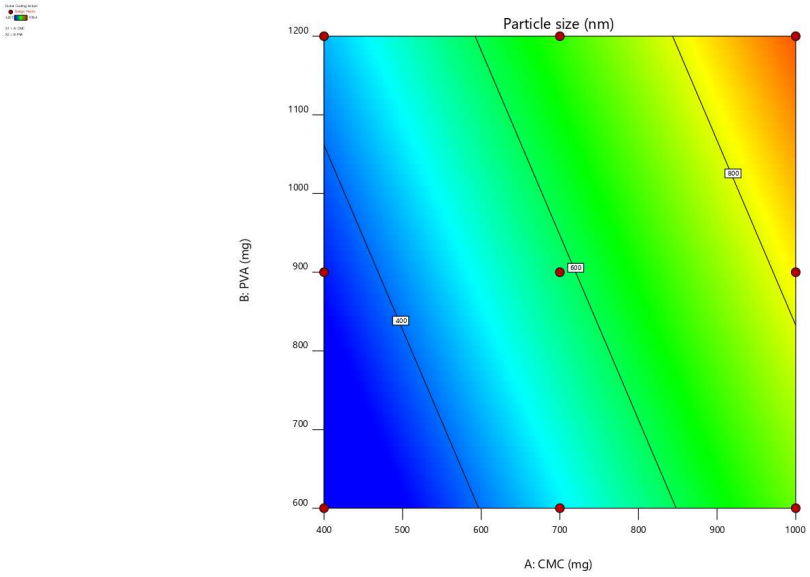

Figure 5: the 2D contour plot of particle size

Table 5: Results of the different models for PDI

Source	Std. Dev.	R^2	Adjusted r^2	Predicted r^2	Press	
Linear	0.0365	0.9410	0.9214	0.8555	0.0196	Suggested
2fi	0.0345	0.9560	0.9296	0.8260	0.0236	
Quadratic	0.0357	0.9718	0.9248	0.6588	0.0462	
Cubic	0.0083	0.9995	0.9959	0.9066	0.0127	Aliased

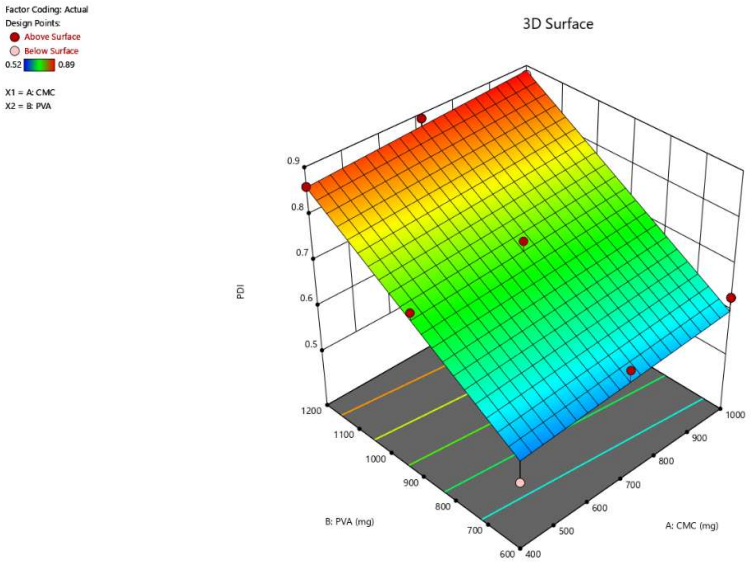

Figure 6: the 3D surface plot of PDI

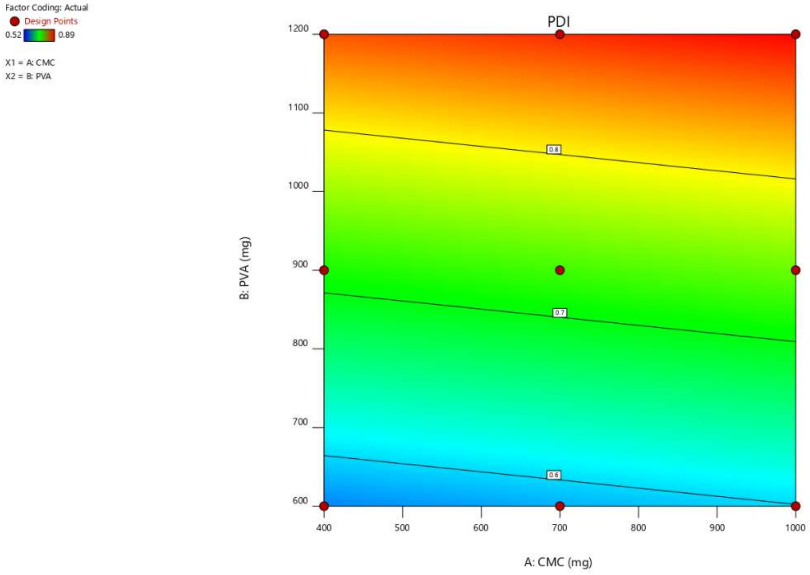

Figure 7: the 2D contour plot of PDI

Table 6: Different models suggested by the software for Entrapment Efficiency

Source	Std. Dev.	R^2	Adjusted r^2	Predicted r^2	Press	
Linear	4.30	0.5799	0.4399	0.0533	250.46	
2fi	4.15	0.6739	0.4782	-0.1355	300.40	
Quadratic	1.06	0.9873	0.9661	0.8726	33.71	Suggested
Cubic	1.23	0.9942	0.9539	-0.0507	277.97	Aliased

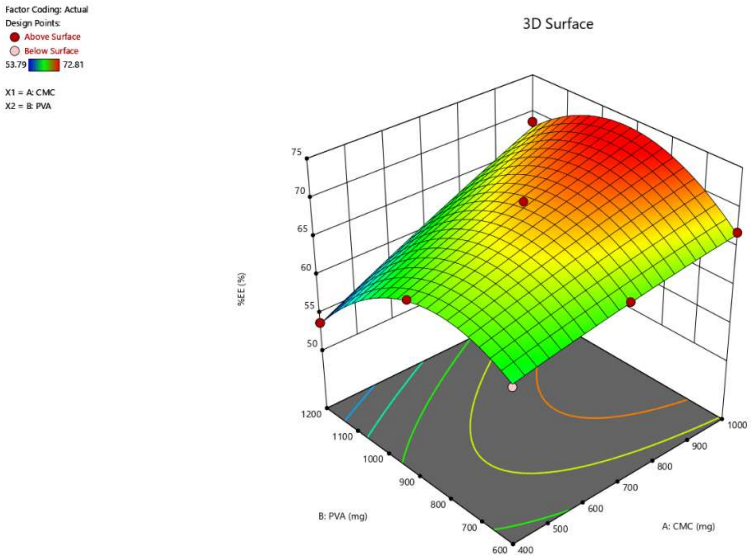

Figure 8: the 3D surface plot of % Entrapment Efficiency

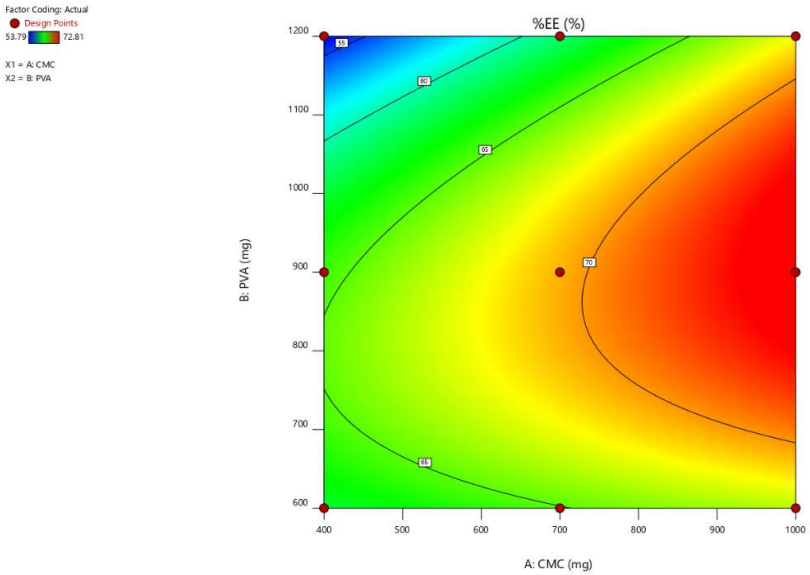

Figure 9: the 2D contour plot of %EE

Results

			Size (d.nm...	% Intensity:	St Dev (d.n...
Z-Average (d.nm):	332.4	Peak 1:	290.9	100.0	166.8
PdI:	0.52	Peak 2:	0.000	0.0	0.000
Intercept:	0.669	Peak 3:	0.000	0.0	0.000
Result quality	Good				

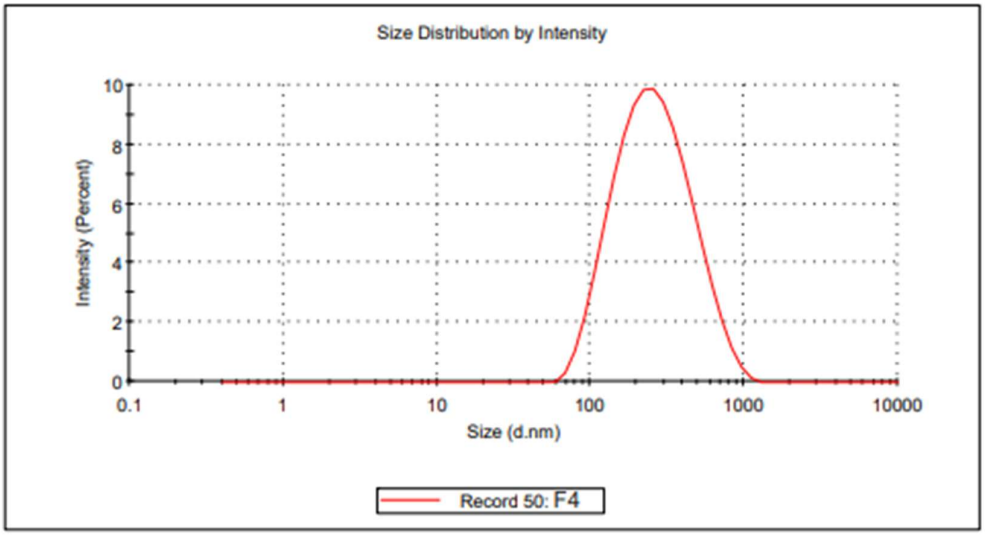

Figure 10: particle size of optimized batch

Results

		Mean (mV)	Area (%)	Width (mV)
Zeta Potential (mV): -15.3	**Peak 1:**	-15.3	100.0	6.96
Zeta Deviation (mV): 6.96	**Peak 2:**	0.00	0.0	0.00
Conductivity (mS/cm): 0.0560	**Peak 3:**	0.00	0.0	0.00

Result quality : Good

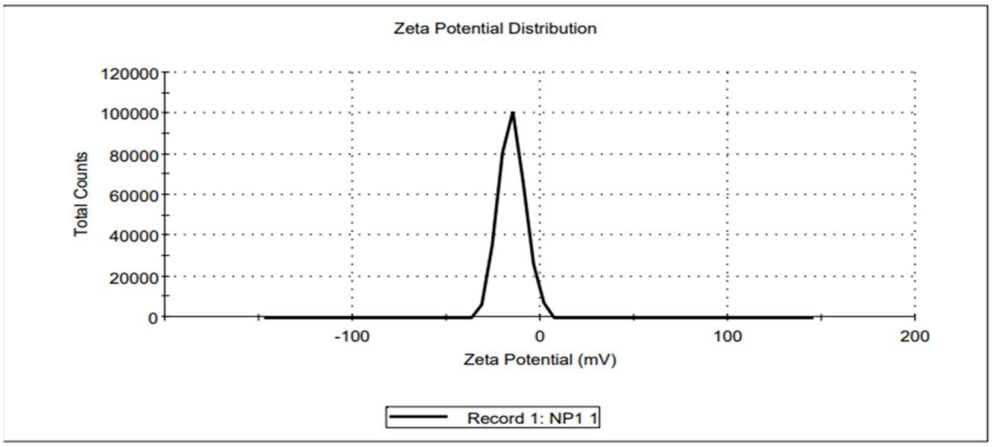

Figure 11: zeta potential of optimized batch

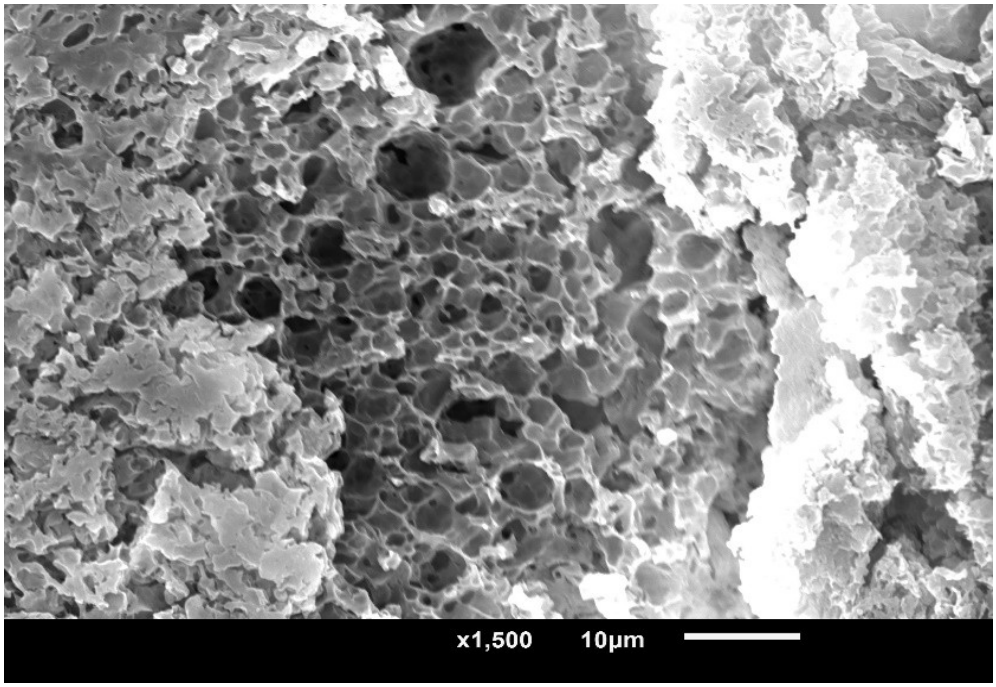

Figure 12: SEM image of optimized batch

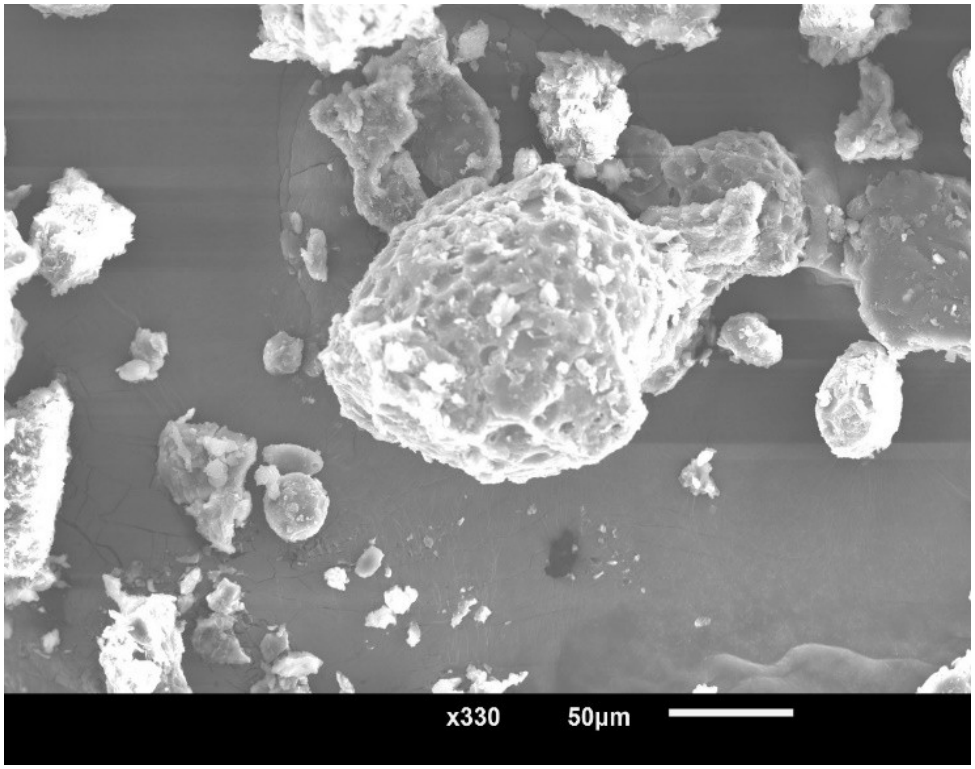

Figure 13: spherical shape of LPZ loaded nanosponge

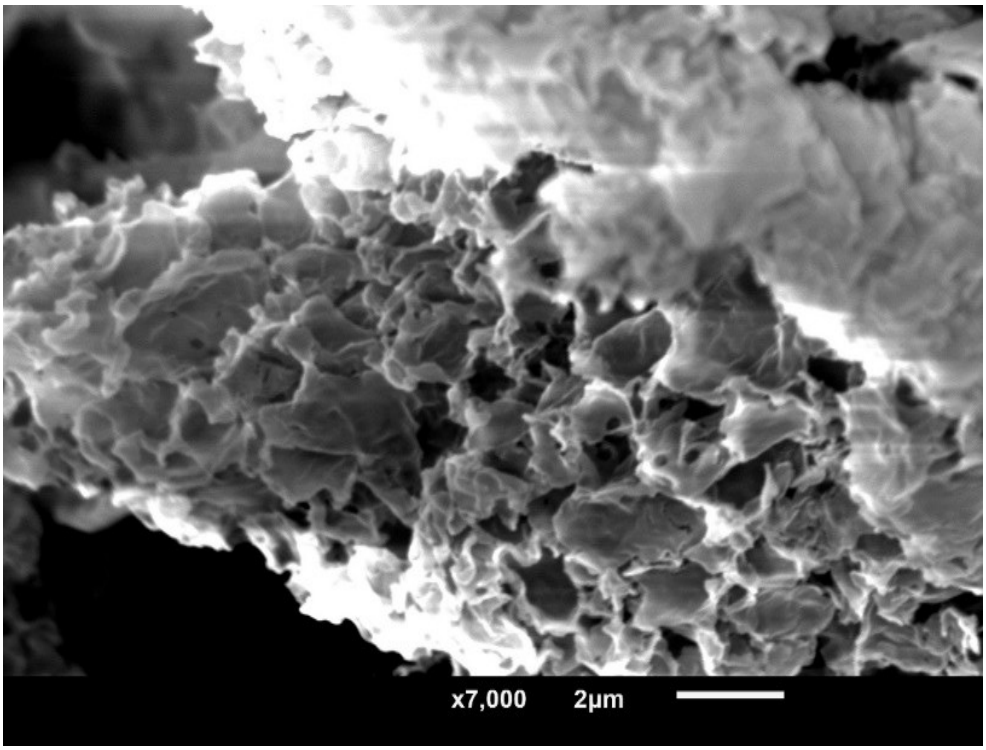

Figure 14: porous structure of LPZ loaded nanosponge

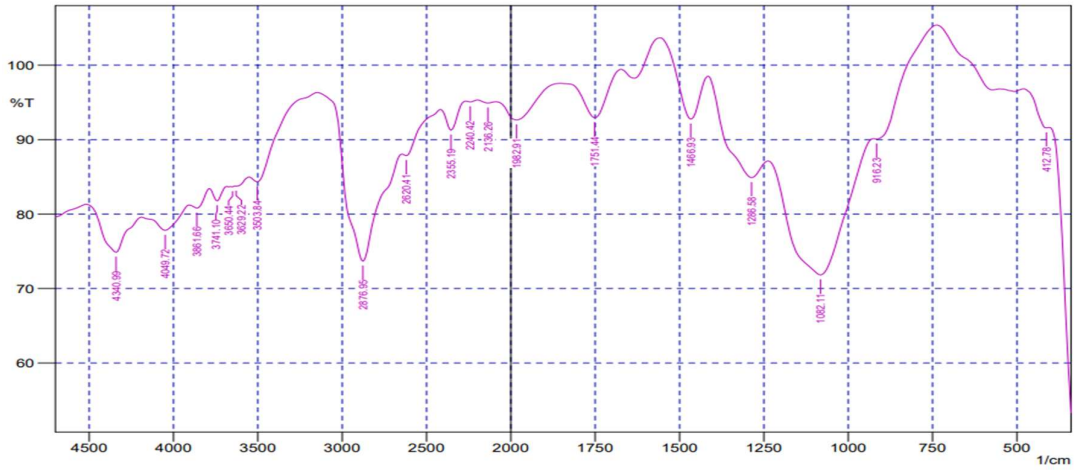

Figure 15: FTIR spectra of drug loaded nanosponge

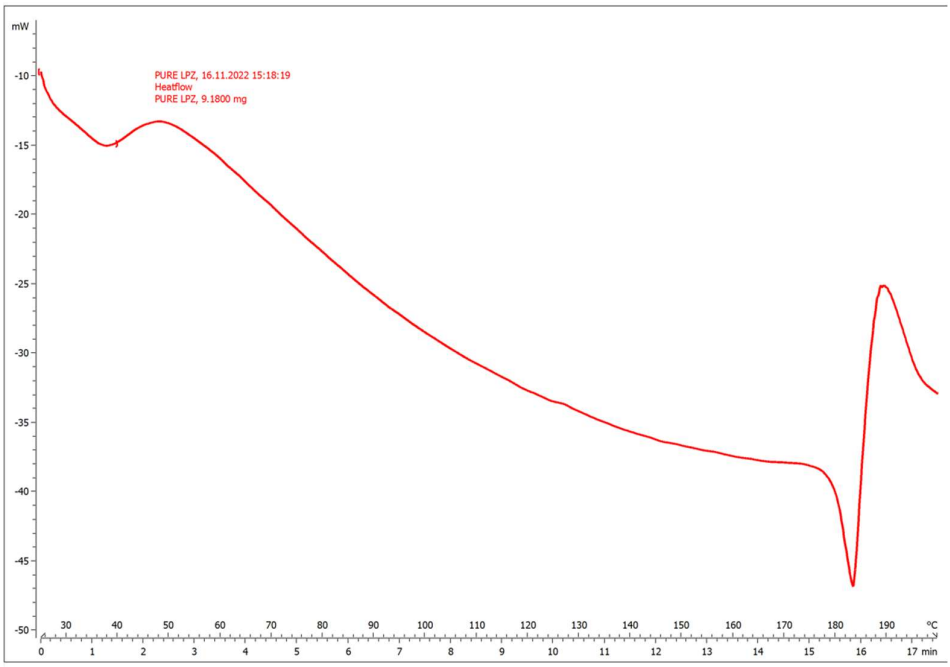

Figure 16: DSC graph of pure LPZ drug

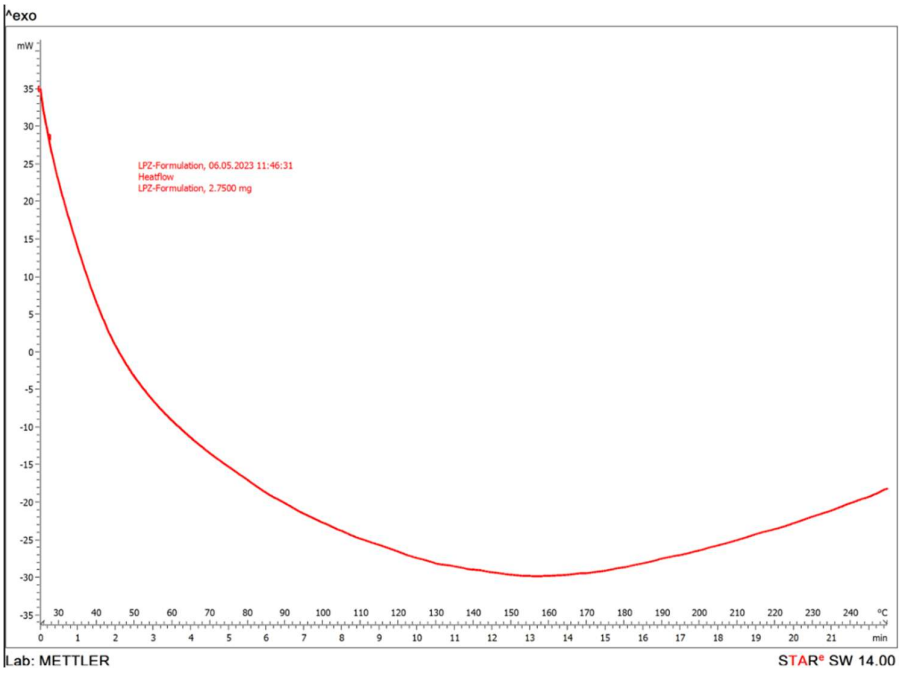

Figure 17: DSC graph of LPZ-loaded nanosponge

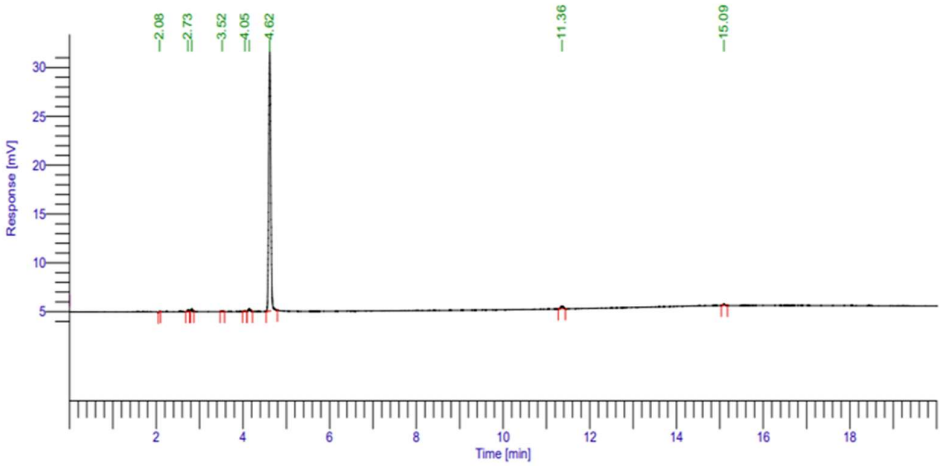

Figure 18: graph of standard Dicholoromethane

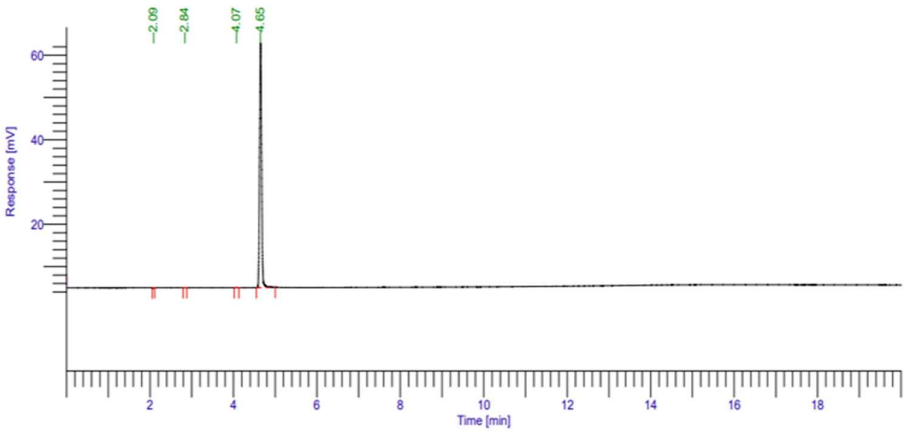

Figure 19: graph of optimized batch

Table 7: Drug release of optimized batch

Time	%CDR
1	10.584±0.52
2	15.754±0.42
3	25.985±0.52
4	45.245±0.54
5	60.214±0.65
6	74.743±0.47
7	80.541±0.32
8	85.245±0.84
9	90.548±0.21
10	95.426±0.63
11	99.452±0.72

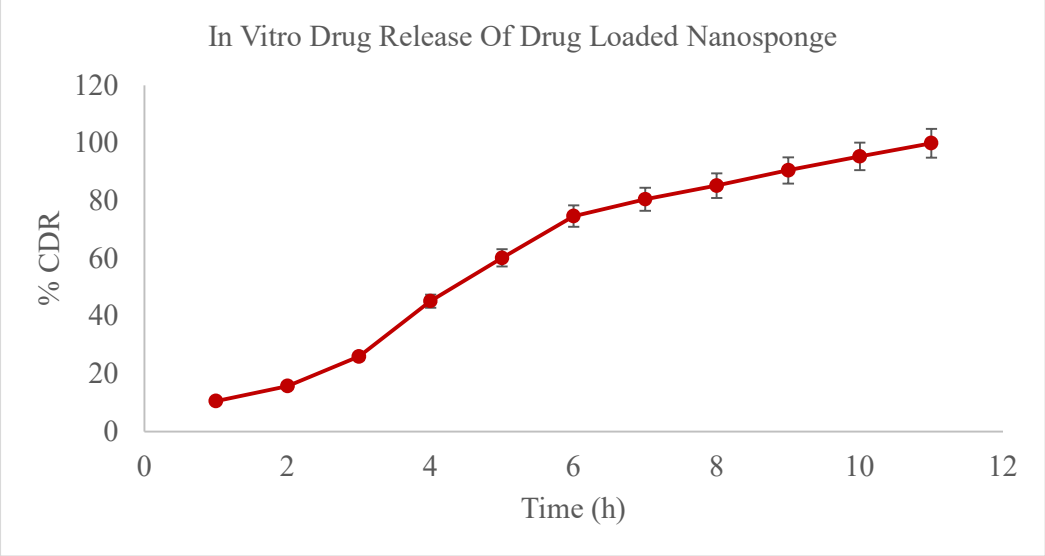

Figure 20: in vitro drug release of LPZ-loaded nanosponge

Table 8: Result table of Drug release of Buccal film

Time	%CDR
1	15.985 ± 0.42
2	31.928 ± 0.11
3	45.925 ± 0.31
4	59.142 ± 0.59
5	60.487 ± 0.38
6	75.847 ± 0.55
7	89.657 ± 0.41
8	98.542 ± 0.65

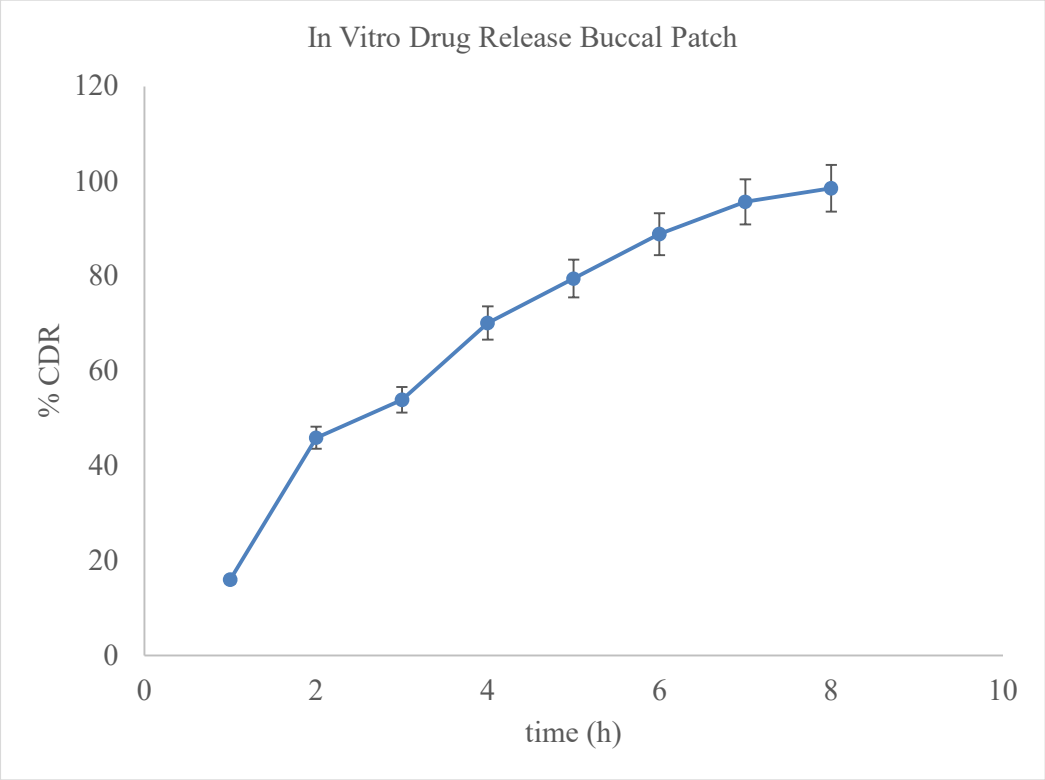

Figure 21: In vitro drug release graph %CDR vs time

CONCLUSION:

The buccal patch formulation of Lansoprazole demonstrated efficient drug delivery, characterized by high purity, effective encapsulation, and a controlled, sustained release profile. These findings indicate the potential suitability of this formulation for clinical applications requiring rapid onset and prolonged therapeutic effects. The consistency and reliability of the data further support the robustness of the formulation and its promising applicability in therapeutic settings.

Declarations:

Funding: No external funding received

Conflicts of interest: no conflict of interest.

Availability of data and materials: Data will be available on request

Ethics approval: Not applicable.

Author contributions: Both authors agreed to work on various aspects of the submitted manuscript. There is no conflict of interest between authors.

Informed consent: Not applicable.

REFERENCES:

[1] Khafagy ES, Abu Lila AS, Sallam NM, Sanad RA, Ahmed MM, Ghorab MM, Alotaibi HF, Alalaiwe A, Aldawsari MF, Alshahrani SM, Alshetaili A. Preparation and Characterization of a Novel Mucoadhesive Carvedilol Nanosponge: A Promising Platform

for Buccal Anti-Hypertensive Delivery. Gels. 2022 Apr 11;8(4):235.

[2] Bhowmik H, Venkatesh DN, Kuila A, Kumar KH. Nanosponges: A review. International journal of applied pharmaceutics. 2018 Jul 7:1-5.

[3] Balakrishna T. Formulation and evaluation of lansoprazole fast dissolving buccal films. Asian Journal of Pharmaceutics (AJP). 2018 Aug 19;12(02).

[4] Pavankumar GV, Ramakrishna V, William GJ, Konde A. Formulation and evaluation of buccal films of salbutamol sulphate. Indian journal of pharmaceutical sciences. 2005;67(2):160-4.

[5] Poynard T, Lemaire M, Agostini H. Meta-analysis of randomized clinical trials comparing lansoprazole with ranitidine or famotidine in the treatment of acute duodenal ulcer. European journal of gastroenterology & hepatology. 1995 Jul 1;7(7):661-5.

[6] Shojaei AH. Buccal mucosa as a route for systemic drug delivery: a review. J Pharm Pharm Sci. 1998 Jan 1;1(1):15-30.

[7] Abruzzo A, Bigucci F, Cerchiara T, Cruciani F, Vitali B, Luppi B. Mucoadhesive chitosan/gelatin films for buccal delivery of propranolol hydrochloride. Carbohydrate polymers. 2012 Jan 4;87(1):581-8.

[8] K J, C KK, P V. A review on peptic ulcer. J Pharm Med H Sci [Internet]. 2022 Jan. 29 [cited 2023 Nov. 24];5(1):19-26.

[9] Francis DJ, Yusuf FS. Development and evaluation of nanosponges loaded extended release tablets of lansoprazole. Universal Journal of Pharmaceutical Research. 2019;4(1):24-8.

[10] Streubel A, Siepmann J, Bodmeier R. Gastroretentive drug delivery systems. Expert opinion on drug delivery. 2006 Mar 1;3(2):217-33.

[11] Kavitt RT, Lipowska AM, Anyane-Yeboa A, Gralnek IM. Diagnosis and treatment of peptic ulcer disease. The American journal of medicine. 2019 Apr 1;132(4):447-56.

[12] Rizvi SS, Akhtar N, Minhas MU, Mahmood A, Khan KU. Synthesis and characterization of carboxymethyl chitosan nanosponges with cyclodextrin blends for drug solubility improvement. Gels. 2022 Jan 12;8(1):55.

[13] The ascension of nanosponges as a drug delivery carrier: preparation, characterization, and applications

[14] Penjuri SC, Ravouru N, Damineni S, Bns S, Poreddy SR. Formulation and evaluation of lansoprazole loaded Nanosponges. Turk. J. Pharm. Sci. 2016 Sep 1;13(3):304-10.